Dual-wavelength digital holographic phase reconstruction based on a polarization-multiplexing configuration

Zhe Wang (王 喆)[1,2], Yifei Chen (陈依菲)[1,2], and Zhuqing Jiang (江竹青)[1,2,*]

[1]*College of Applied Sciences, Beijing University of Technology, Beijing 100124, China*
[2]*Institute of Information Photonics Technology, Beijing University of Technology, Beijing 100124, China*
**Corresponding author: zhqjiang@bjut.edu.cn*

Received August 31, 2015; accepted November 26, 2015; posted online January 6, 2016

We present a polarization-multiplexing off-axis Mach–Zehnder configuration for dual-wavelength digital holography to achieve phase imaging in one shot. In this configuration, two orthogonal linear-polarized waves with respect to different wavelengths are employed to record respective holograms synchronously, where two recording waves transmit independently through the same optical paths of the interferometer, and by installing two analyzer polarizers each to filter off either of two wavelengths, and filtering through the other, the holograms are acquired, respectively, by a pair of CCDs at the same time. The unwrapped phase image of a grating with groove depth 7.1 μm is retrieved via spatial frequency filtering.

OCIS codes: 090.1995, 090.5694.
doi: 10.3788/COL201614.010008.

Digital holography is a technique that can reconstruct the phase images of an object by the acquisition of the object's holograms with a CCD camera and numerical reconstruction imaging via simulation of the hologram's diffraction imaging process[1–7]. The phase reconstruction imaging of digital holography using a single wavelength is just suitable to handle smooth profiles and step heights less than the wavelength. While a target object is of larger optical thickness than the recording wavelength in digital holography, its phase image typically contains 2π discontinuities, referred to as phase wrapping. Thus, the actual phase image of the object has to be retrieved from its wrapping phase image by using numerical phase unwrapping algorithms[8]. The numerical phase unwrapping in single-wavelength digital holography may induce some error if the target structure has a high aspect ratio. However, dual-wavelength digital holography may complete the phase imaging for a target object of larger or abrupt height variance via careful choice of two wavelengths. It can retrieve the phase image just by yielding a synthetic phase map free of 2π discontinuities from two holograms recorded with different wavelengths, without the need of numerical phase unwrapping in phase reconstruction[9,10]. Since dual-wavelength digital holography has the advantage of imaging a height step object without unwrapping, various recording configurations and phase reconstruction based on dual-wavelength digital holography have been actively researched in recent years[11–15].

In this Letter, a polarization-multiplexing off-axis Mach–Zehnder configuration of dual-wavelength digital holography is proposed for the reconstruction of quantitative phase images in which two orthogonal linear-polarized waves with respect to different wavelengths pass through the same off-axis interferometer to record the holograms. According to the independent propagation of two linear-polarized waves orthogonal to one another, two different wavelength lasers, respectively, to a *p*-polarization and a *s*-polarization can transmit together in the same optical path of the interferometer without any optical interference between them. The two holograms from the different wavelengths can be synchronously acquired with a pair of CCDs by installing one polarizer with its polarization state parallel to the *s*-polarization and the other polarizer parallel to the *p*-polarization, each in front of the CCDs. Both polarizers act as a filter through one pair of interference beams among the two wavelengths to form one interferogram and filtering off the other. Thus, the holograms of dual-wavelength digital holography can be captured in one shot based on this polarization-multiplexing configuration. The presented configuration provides the capabilities of polarization-multiplexing transmission for two separate wavelengths and of automatic spatial-frequency filtering in dual-wavelength digital holography. Furthermore, it is more compact because one interferometer path is simultaneously provided as two polarization channels. The phase image of a phase-only grooved grating is retrieved with relevant spatial frequency filtering and dual-wavelength numerical reconstruction in the presented polarization-multiplexing optical configuration.

For dual-wavelength digital holographic imaging, two interferograms formed with two pairs of the interference beams of different wavelengths are required to be recorded by image sensors, such as CCD cameras, which are referred to as the digital holograms corresponding to the separate wavelengths. After obtaining two independent phase images from respective digital holograms, a synthetic phase image can be yielded with the subtraction of the two single-wavelength phase images. Thus, the

unwrapped phase image of a target object is completely achieved according to the synthetic phase image. For a target object of transmission topography, the synthetic phase distribution of two single-wavelength phase images can be typically expressed as

$$\Delta\varphi = \varphi_1 - \varphi_2 = 2\pi nh\left(\frac{1}{\lambda_1} - \frac{1}{\lambda_2}\right) = \frac{2\pi nh}{\Lambda}, \qquad (1)$$

where φ_1 and φ_2 denote the reconstructed phases with respective to λ_1 and λ_2, n and h are the refractive index and the topographic height of the object, and Λ is referred to as the synthetic wavelength of λ_1 and λ_2.

In the presented dual-wavelength digital holographic configuration, two holograms with different wavelengths are formed with the p-polarized interference beams of wavelength λ_1 and the s-polarized beams of wavelength λ_2 based on the optical configuration of interferometer. The two holograms can be recorded with two same-model CCD cameras at same time, since two polarizers oriented parallel with the p-polarization and the s-polarization have been placed in front of the CCDs for filtering out the interference beams mismatched with the polarizer's orientation.

A polarization-multiplexing off-axis configuration for dual-wavelength digital holography is shown in Fig. 1. The 671 nm laser beam is adjusted to the p-polarized (parallel to the optical plane) via half-wave plate HWP1 placed behind beam splitter (BS1) and then transmits through polarizing beam splitter (PBS). The 656 nm laser beam becomes s-polarized (perpendicular to the optical plane) after it is reflected by the PBS. The p-polarized 671 nm beam and the s-polarized 656 nm beam are combined via the PBS, and then go together into the optical arrangement of a Mach–Zehnder interferometer in which the different polarization beams share the object path and the reference path. According to off-axis holographic recording, an off-axis interference angle between the propagation directions of an object beam and a reference beam is

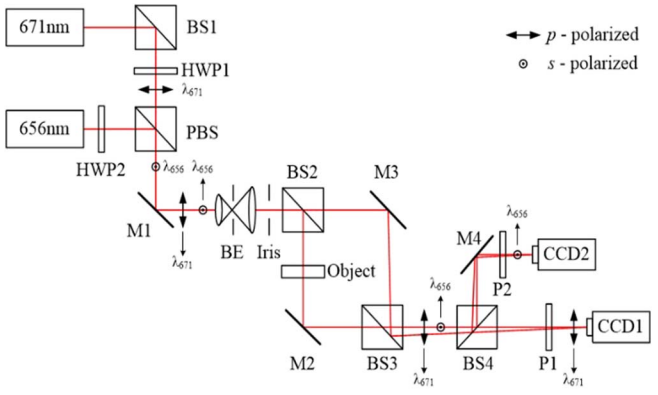

Fig. 1. Schematic of a polarization-multiplexing off-axis dual-wavelength digital holographic system, HWP: half-wave plate. M: mirror. BE: beam-expander. Object: a grooved grating. P: polarizer.

typically required. By means of the shared-path propagation in the interferometer, the two pairs of interference beams readily build almost the same off-axis interference angle.

For using the PBS it is necessary to obtain both a p-polarization wave and an s-polarization wave in this polarization-multiplexing configuration for dual-wavelength digital holography. Herein, the PBS functions to convert the linear polarization state of the 656 nm wave into s-polarization and to keep the p-polarization 671 nm wave passing through. In particular, it is required for converting the 656 nm laser wave to the s-polarization wave, because the output beam of the 656 nm laser typically contains several different modes. In the experiment, replacing the PBS with a BS causes a drastic decline of image quality.

As we know, one-term phase distortion caused by the off-axis angle typically exists in digital holographic imaging. In most optical setups, the off-axis interference angles of the different wavelength beams in real-time dual-wavelength digital holography are not the same as each other unless they are adjusted quite carefully in hard work. Fortunately, in the presented scheme, the difference of the off-axis angles can be naturally ignored due to the shared-path propagation of two wavelengths. Furthermore, the effect of dispersion on off-axis angles is negligible because two wavelengths are quite close. Thus, the polarization-multiplexing configuration with the shared-path transmission has the advantage that one-term phase distortion of the reconstructed phase image is almost eliminated in dual-wavelength phase unwrapping.

After passing through the interferometer, the object beams and the reference beams of the 671 nm and 656 nm wavelengths can form their interferograms at the same propagation distance. The BS4 is used to split the combined interference waves into two parts that are incident into polarizers P1 and P2. The p-polarized 671 nm interference wave can pass through polarizer P1 with horizontal polarization, and the s-polarized 656 nm interference wave can pass through polarizer P2 with vertical polarization. Meanwhile, the p-polarized 671 nm wave and the s-polarized 656 nm wave are filtered off by polarizers P2 and P1, respectively. Thus, the off-axis interferograms of the 671 and 656 nm interference waves, termed as the digital holograms, can be built on the sensor surfaces of CCD1 and CCD2, respectively, in one shot.

The optical length of the 671 nm beam from BS4 to CCD1 is nearly the same as that of the 656 nm beam from BS4 to CCD2, which is required to achieve the same-time recording. Because of off-axis digital holographic recording, there is the off-axis angle between the reference beam and the object beam. The angles between the object and the reference beams incident onto the surfaces of two CCD cameras are equal. Thus, according to the presented optical configuration, the automatic filtering of the spatial frequency spectrum and the phase reconstruction for the dual-wavelength holograms can be realized.

For the phase reconstruction of dual-wavelength digital holography, the phase images with respect to two single-wavelength holograms are achieved. First, the spatial frequency distribution of the respective holograms should be obtained by Fourier transform. The spatial frequency filtering of the holograms can be carried by a numerical bandpass filter in the spatial frequency domain. Typically, the operations of spatial frequency filtering on two single-wavelength holograms in dual-wavelength digital holography are individually performed[16]. For the real-time imaging applications of dual-wavelength digital holography, such twice running of the spatial frequency filtering is actually time consuming, particularly if there are many holograms to be handled. Fortunately, based on the presented polarization-multiplexing configuration, there is a relationship between both the first-order (the order +1) spectra in the spatial frequency domain of two holograms with their recording wavelengths. The centers of the order +1 spectra in the spatial frequency domain of the holograms can be located according to two recording wavelengths as

$$\frac{B_1}{B_2} = \frac{\lambda_2}{\lambda_1}, \tag{2}$$

where B_1 and B_2 denote the carrier frequencies of two holograms with respect to wavelengths λ_1 and λ_2, which are the distances from the centers of the order +1 to the center of the Fourier spectrum in the spatial frequency domain, respectively. Equation (2) is deduced from the relationship of the angular spectrums of the two holograms. According to Eq. (2), if the center location of the order +1 spectrum of either of two wavelengths is determined, the center of the order +1 of another wavelength is readily calculated. Thus, the phase reconstruction based on the angular-spectrum filtering can be efficiently realized in dual-wavelength off-axis digital holography based on the presented polarization-multiplexing configuration.

In the experimental setup shown in Fig. 1, two laser waves at wavelengths of 671 and 656 nm are used for recording the dual-wavelength digital holograms. According to Eq. (1), the synthetic wavelength of 671 and 656 nm is about 29.35 μm. Two identical model CCDs are employed. The sensor size of the CCDs is 1384 pixels× 1036 pixels, and the pixel size is 6.45 μm × 6.45 μm. The polarizers P1 and P2 are placed in front of CCD1 and CCD2, and are adjusted to horizontal-polarized and vertical-polarized orientations, respectively, so that the polarizer P1 filters off the 656 nm beams and the polarizer P2 filters off the 671 nm beams. Thus, CCD1 and CCD2 record the interference fringe patterns (or digital holograms) that are generated with the interference waves at the wavelengths 671 and 656 nm, respectively. A grooved grating with groove depth 7.1 μm as a target object is used to demonstrate the dual-wavelength phase reconstruction in the presented polarization-multiplexing configuration of dual-wavelength digital holography.

First, two single-wavelength holograms of the grooved grating with the *p*-polarized 671 nm wave and the *s*-polarized 656 nm wave are synchronously acquired by CCD1 and CCD2, respectively, as shown in Figs. 2(a) and 2(b). In the reconstruction procedure, the phase map of the target grating is numerically retrieved with the dual-wavelength unwrapping method. Figures 2(c) and 2(d) show the Fourier spectrum distributions of two 671 nm and 656 nm holograms in which the red boxes represent their filtering windows. As shown in Figs. 2(e) and 2(f), two phase images of the single-wavelength holograms still consist of a wrapping phase therein, which are retrieved according to the angular spectrum theory of scalar diffraction. Then, the synthetic phase image is obtained directly

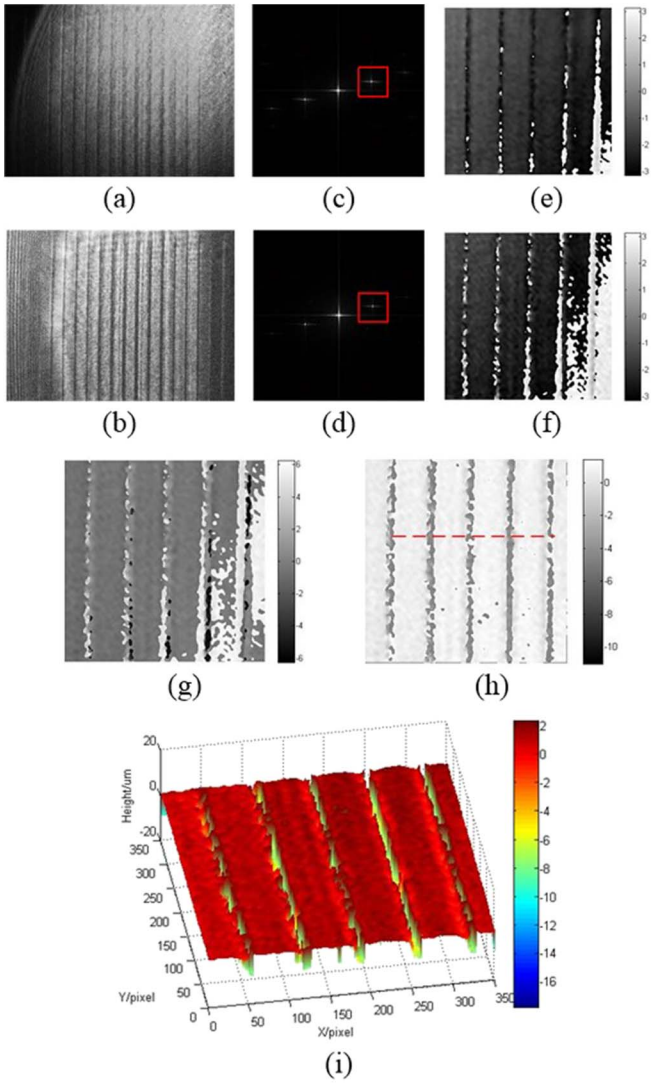

Fig. 2. Reconstruction imaging of the polarization-multiplexing dual-wavelength holography, (a) 671 nm hologram, (b) 656 nm hologram, (c) spatial-frequency spectrum of 671 nm hologram, (d) spatial-frequency spectrum of 656 nm hologram, (e) wrapped phase image for 671 nm, (f) wrapped phase image for 656 nm, (g) synthetic phase image, (h) synthetic phase map with phase compensation, and (i) 3D reconstruction map of the height distribution of the object.

by subtraction of the 656 and 671 nm phase images according to Eq. (1), shown in Fig. 2(g). Based on the principle of dual-wavelength digital holographic imaging, the phase compensation of 2π is applied on the synthetic phase to reconstruct the actual phase map of a target object, when the value of synthetic phase is less than zero. Further, the actual phase map of the grooved grating with 2π phase compensation is shown in Fig. 2(h), and its 3D phase map is shown in Fig. 2(i).

When the screen size and pixel size of the CCD camera are fixed, the difference in the imaging scale of two wavelengths can be considered as chromatic aberrations. In dual-wavelength digital holography, the chromatic aberrations act as the difference of phase maps. The subtraction of the wavelength-different phase maps requires an achromatic setup. Otherwise, numerical image resizing is needed[10].

In the phase reconstruction, the image registration for the two holograms should be conducted to make them have accurate alignment because the single-wavelength holograms are recorded with two CCDs. The image registration is realized based on the phase-correlation of the holograms. After performing the image registration for the holograms, two single-wavelength phase images can be retrieved from their holograms by the numerical reconstruction of diffraction imaging. Further, by calculating the synthetic phase and finishing the phase compensation to it, the actual phase image of the groove grating can be reconstructed completely.

Figure 3 shows the cross-sectioned profile of groove depth of the grating along a red dash line in Fig. 2(h). The 3D map of the height distribution of the grooved grating with refractive index 1.49 is rebuilt from the phase reconstruction map of Fig. 2(h).

The unevenness of the local maxima and minima on the measured height profile shown in Fig. 3 is attributed to some noises, such as fixed pattern noise (pixel to pixel sensitivity variation), inherent noise due to the spatial filtering window and the 2D-FFT process[17], and diffraction noise caused by the diffraction of groove edges of the grating, which typically occurs for an object having cliffy

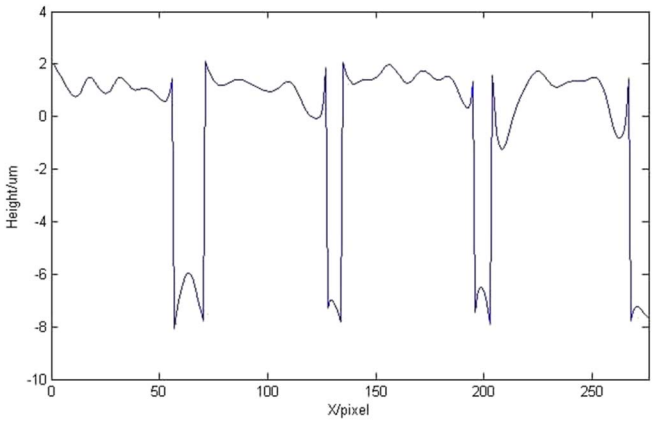

Fig. 3. Reconstructed height profile of the grooved grating.

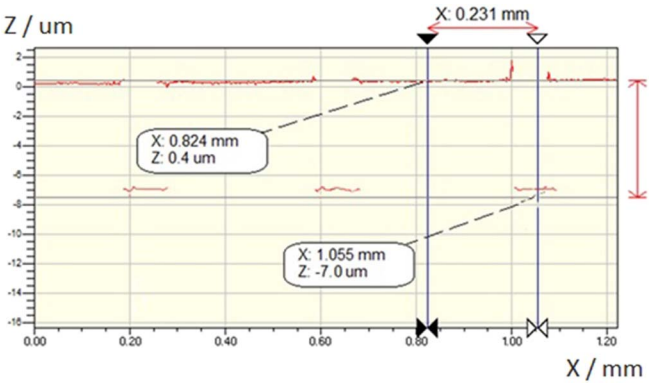

Fig. 4. Grooved depth measured by the profile meter (WYKO NT1100 manufactured by Veeco, USA).

edges or steeps in digital holographic imaging. In some reported works, the unevenness is smoothed by applying the root mean square (RMS) method[12,17]. The noises may not show up via shifting the reconstruction distance away from the actual distance of the object when performing numerical retrieval imaging, but it is at the expense of the loss of edge information. The speckle noise in digital holography can also be reduced by using a spatial light modulator with a nonlocal means algorithm[18].

In addition, it should be mentioned that, even though the refractive index of PMMA (polymethyl methacrylate) material is wavelength dependent, the difference in the refractive index of PMMA material is less than 5×10^{-4}. Specifically, for the wavelength difference of 15 nm between the 671 and 656 nm laser waves used here in this configuration, the estimated relative error of the topographic height in the grating in this transmission geometry is less than 1.46%, so the influence of wavelength dependence is negligible.

The experimental data is verified by using a profile meter (WYKO NT1100 manufactured by Veeco, USA) to measure the surface profile of the grating. The grooved depth measured by the profile meter is 7.4 μm, as shown in Fig. 4. The result shows that the surface profile retrieved by dual-wave digital holography is in good agreement with that exhibited by a profile meter. It demonstrates that the reconstructed phase distribution in this polarization-multiplexing configuration is reliable for surface profile measurement.

Thus, based on a polarization-multiplexing off-axis Mach–Zehnder configuration for dual-wavelength digital holography, the phase reconstruction of a grooved grating is achieved by one-shot capture of two single-wavelength holograms and the relevance relation of the spatial frequency spectrum of the two holograms.

In conclusion, the presented polarization-multiplexing configuration of dual-wavelength digital holography is employed to achieve unwrapping phase imaging. The dual-wavelength holographic system has the features that two recording waves can share the same interferometer optical path to transmit independently due to their

polarizations being perpendicular to each other, and then by installing each of the proper polarizers in front of the CCDs to filter off either of two wavelengths and filtering through the other, each of the holograms according to their different wavelengths can be acquired by a pair of CCDs at the same time. Since the two wavelengths pass through almost the same optical path, the phase distortion of the off-axis system in two phase maps are nearly identical, which will greatly simplify the process of phase distortion removal. Further, two holograms are recorded separately at the same time, with respect to their wavelengths, so the interplay between the holograms in the procedure of spectrum filtering and image reconstruction does not needed to be considered. Moreover, this polarization-multiplexing configuration is compact and effective, so it can be easily extended to phase imaging of three or more wavelengths that will further expand the imaging scale, and will be readily compacted in future practical applications.

Experimentally, the phase retrieval of a target grating is demonstrated in this system. The dual-wavelength digital holograms are recorded, respectively, with the *p*-polarized 671 nm interference beams and the *s*-polarized 656 nm interference beams at the same time. The phase image of a grooved grating and its height profile of 7.1 μm are reconstructed by using the relevance relationship of the spatial frequency spectrum of two holograms based on the presented configuration. The unwrapping phase imaging is dependent on the value of the synthetic wavelength in the dual-wavelength digital holographic imaging system. Although we just show the reconstructed image of a grating of grooved depth 7.1 μm, the topographic height less than 29.35 μm also can be retrieved with an unwrapping phase by using the wavelengths of 656 and 671 nm according to the principle of dual-wavelength unwrapping phase reconstruction.

This configuration has the merits of compact structure, because one interferometer path is simultaneously provided as two polarization channels, and of fast numerical reconstruction. This work can be further developed into a real-time phase imaging solution as cooperation with the automatic spectral filtering algorithm for off-axis dual-wavelength digital holographic imaging.

This work was supported by the Beijing Natural Science Foundation Program and the Scientific Research Key Program of Beijing Municipal Commission of Education of China under Grant No. KZ201310005007.

References

1. J. W. Goodman and R. W. Lawrence, Appl. Phys. Lett. **11**, 77 (1967).
2. U. Schnars and W. Jüptner, Appl. Opt. **33**, 179 (1994).
3. T. M. Kreis, M. Adams, and W. P. O. Jüptner, Proc. SPIE **3098**, 224 (1997).
4. E. Cuche, F. Bevilacqua, and C. Depeursinge, Opt. Lett. **24**, 291 (1999).
5. E. Cuche, P. Marquet, and C. Depeursinge, Appl. Opt. **38**, 6994 (1999).
6. T. Colomb, P. Dahlgren, D. Beghuin, E. Cuche, P. Marquet, and C. Depeursinge, Appl. Opt. **41**, 27 (2002).
7. P. Marquet, B. Rappaz, P. J. Magistretti, E. Cuche, Y. Emery, T. Colomb, and C. Depeursinge, Opt. Lett. **30**, 468 (2005).
8. M. Servin, J. L. Marroquin, D. Malacara, and F. J. Cuevas, Appl. Opt. **37**, 1917 (1998).
9. J. Gass, A. Dakoff, and M. K. Kim, Opt. Lett. **28**, 1141 (2003).
10. D. Parshall and M. K. Kim, Appl. Opt. **45**, 451 (2006).
11. J. Kuhn, T. Colomb, and F. Montfort, Opt. Exp. **15**, 7231 (2007).
12. D. G. Abdelsalam, R. Magnusson, and D. Kim, Appl. Opt. **50**, 3360 (2011).
13. J. Min, B. Yao, and M. Zhou, J. Opt. **16**, 125409 (2014).
14. P. Bergström, D. Khodadad, E. Hällstig, and M. Sjödahl, Appl. Opt. **53**, 123 (2014).
15. Y. Lee, Y. Ito, and T. Tahara, Opt. Express **39**, 2374 (2014).
16. E. Stoykova, H. Kang, and J. Park, Chin. Opt. Lett. **12**, 060013 (2014).
17. D. G. Abdelsalam and D. Kim, Opt. Commun. **285**, 233 (2012).
18. J. Leng, X. Sang, and B. Yan, Chin. Opt. Lett. **12**, 040301 (2014).